

Reduction of Ripple in the Bidirectional DC-DC Converter with the Coupled Inductor

K.C.Ramya¹, V.Jegathesan²

Research Scholar, Department of Electrical and Electronics Engineering, Karunya University, Coimbatore, India¹

Associate Professor, Department of Electrical and Electronics Engineering, Karunya University, Coimbatore, India²

ABSTRACT: This work deals with reduction of ripple in the bidirectional DC-DC converter. This Converter has the ability to transfer the energy in both the directions. This converter is designed, modeled and simulated using MATLAB SIMULINK and the results are presented. The Pi-filter is proposed at the output to reduce the peak to peak ripple. The simulation results with R-load and DC-Motor load are presented.

KEYWORDS: Bidirectional DC-DC converter, Coupled Inductor, Filter.

I. INTRODUCTION

Bidirectional DC-DC converters (BDC) are used to transfer the power between two DC sources in either direction. These converters are widely used in applications, such as hybrid electric vehicle energy systems [1]–[4], uninterrupted power supplies [5], [6], fuel-cell hybrid power systems [7]–[10], photovoltaic hybrid power systems [11], [12], and battery chargers [13]–[15]. Many bidirectional DC-DC converters have been researched. The bidirectional DC-DC flyback converters are more attractive due to simple structure and easy control [2], [16], [17]. However, these converters suffer from high voltage stresses on the power devices due to the leakage inductor energy of the transformer. In order to recycle the leakage inductor energy and to minimize the voltage stress on the power devices, some literature present the energy regeneration techniques to clamp the voltage stress on the power devices and to recycle the leakage inductor energy [18], [19]. Some literatures research the isolated bidirectional DC-DC converters, which include the half-bridge [8], [9], [20], [21] and full-bridge types [13], [22]. These converters can provide high step-up and step-down voltage gain by adjusting the turns ratio of the transformer.

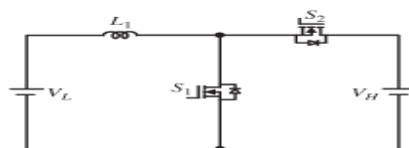


Fig.1: Conventional BDC Boost/Buck Converter

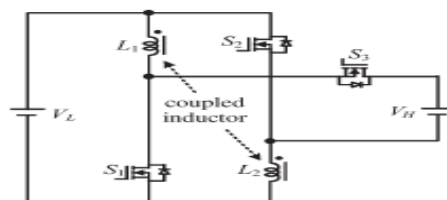


Fig.2: Proposed Bidirectional DC-DC Converter

For non-isolated applications, the non-isolated bidirectional DC-DC converters, which include the conventional boost/buck [1], [5], [12], [14], multilevel [4], three-level [10], sepic/zeta[23], switched capacitor [24], and coupled inductor types [25], are presented. The multilevel type is a magnetic less converter, but 12 switches are used in this converter. If higher step-up and step-down voltage gains are required, more switches are needed. This control circuit becomes more complicated. In the three-level type, the voltage stress across the switches on the three-level type is only half of the conventional type. However, the step-up and step-down voltage gains are low. Since the sepic/zeta type is a

International Journal of Innovative Research in Science, Engineering and Technology

(An ISO 3297: 2007 Certified Organization)

Vol. 4, Issue 2, February 2015

combination of two power stages, the conversion efficiency will be decreased. The switched capacitor and coupled inductor types can provide high step-up and step-down voltage gains. However, their circuit configurations are complicated. Fig.1 shows the conventional bidirectional DC-DC boost/buck converter which is simple structure and easy control. However, the step-up and step-down voltage gains are low.

A modified DC-DC boost converter is presented [26]. The voltage gain of this converter is higher than the conventional DC-DC boost converter. Based on this converter, a novel bidirectional DC-DC converter is proposed [27], as shown in Fig. 2. The proposed converter employs a coupled inductor with same winding turns in the primary and secondary sides. Compared to the proposed converter and the conventional bidirectional boost/buck converter, the proposed converter has the following advantages: 1) Higher step-up and step-down voltage gains and 2) lower average value of the switch current under same electric specifications. The following sections will describe the operating principles and steady-state analysis for the step-up and step-down modes. In order to analyze the steady-state characteristics of the proposed converter, some conditions are assumed: The on-state resistance $R_{DS(ON)}$ of the switches and the equivalent series resistances of the coupled inductor and capacitors are ignored; the capacitor is sufficiently large; and the voltages across the capacitor can be treated as constant.

The above literature does not deal with ripple reduction using Pi-filter. This work proposes Pi-filter for ripple reduction.

II. STEP-UP MODE

The proposed converter in step-up mode is shown in Fig.3. The pulse width modulation (PWM) technique is used to control the switches S_1 and S_2 simultaneously.

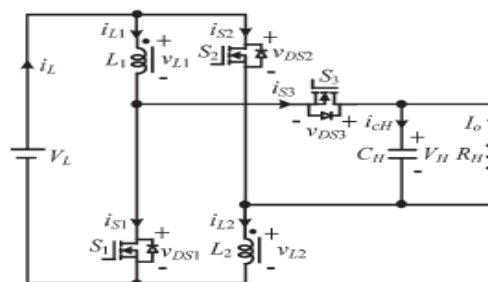


Fig.3: Proposed converter in step-up mode

The switch S_3 is the synchronous rectifier. Since the primary and secondary winding turns of the coupled inductor is same, the inductance of the coupled inductor in the primary and secondary sides are expressed as

$$L_1 = L_2 = L \quad (1)$$

Thus, the mutual inductance M of the coupled inductor is given by

$$M = k\sqrt{L_1 L_2} = kL \quad (2)$$

where k is the coupling coefficient of the coupled inductor.

The voltages across the primary and secondary windings of the coupled inductor are as follows:

$$v_{L1} = L_1 \frac{di_{L1}}{dt} + M \frac{di_{L2}}{dt} = L \frac{di_{L1}}{dt} + kL \frac{di_{L2}}{dt} \quad (3)$$

$$v_{L2} = M \frac{di_{L1}}{dt} + L_2 \frac{di_{L2}}{dt} = kL \frac{di_{L1}}{dt} + L \frac{di_{L2}}{dt}. \quad (4)$$

The operating principles and steady-state analysis of CCM are described as follows,

CCM Operation - Mode 1: During this time interval $[t_0, t_1]$, S_1 and S_2 are turned on and S_3 is turned off. The energy of the low-voltage side V_L is transferred to the coupled inductor. Meanwhile, the primary and secondary windings of the coupled inductor are in parallel. The energy stored in the capacitor C_H is discharged to the load. Thus, the voltages across L_1 and L_2 are obtained as,

$$v_{L1} = v_{L2} = V_L \quad (5)$$

International Journal of Innovative Research in Science, Engineering and Technology

(An ISO 3297: 2007 Certified Organization)

Vol. 4, Issue 2, February 2015

Substituting (3) and (4) into (5), yielding

$$\frac{di_{L1}(t)}{dt} = \frac{di_{L2}(t)}{dt} = \frac{V_L}{(1+k)L}, \quad t_0 \leq t \leq t_1. \quad (6)$$

Mode 2: During this time interval $[t_1, t_2]$, S_1 and S_2 are turned off and S_3 is turned on. The low-voltage side V_L and the coupled inductor are in series to transfer their energies to the capacitor C_H and the load. Meanwhile, the primary and secondary windings of the coupled inductor are in series. Thus, the following equations are found to be

$$i_{L1} = i_{L2} \quad (7)$$

$$v_{L1} + v_{L2} = V_L - V_H \quad (8)$$

Substituting (3), (4), and (7) into (8), yielding

$$\frac{di_{L1}(t)}{dt} = \frac{di_{L2}(t)}{dt} = \frac{V_L - V_H}{2(1+k)L}, \quad t_1 \leq t \leq t_2. \quad (9)$$

By using the state-space averaging method, the following equation is derived from (6) and (9):

$$\frac{DV_L}{(1+k)L} + \frac{(1-D)(V_L - V_H)}{2(1+k)L} = 0. \quad (10)$$

Simplifying (10), the voltage gain is given as

$$G_{CCM(step-up)} = \frac{V_H}{V_L} = \frac{1+D}{1-D}. \quad (11)$$

III. SIMULATION RESULTS

The circuit diagram for boost mode is shown in Fig.4(a). The power output is measured by multiplying the output voltage and the output current. Load voltage and load current are measured using voltage and current blocks respectively. The following are the assumptions made in simulation studies.

- Internal resistance of the source is neglected.
- Resistance of the coupled inductor is neglected.
- ESR of the capacitor is neglected.

The simulation parameters for boost mode with C-filter are as follows:

Coupled Inductor = 1 mH ; C-filter, $C_O = 400\mu\text{F}$ and Resistance, $R_O = 11\Omega$.

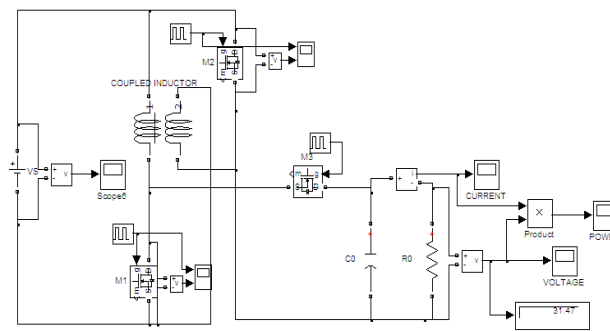


Fig. 4(a) : Circuit Diagram for Boost Mode with C-Filter

DC input voltage of 15V is shown in Fig.4(b). The switching voltage and the voltage across the MOSFET are shown in Fig.4(c).

International Journal of Innovative Research in Science, Engineering and Technology

(An ISO 3297: 2007 Certified Organization)

Vol. 4, Issue 2, February 2015

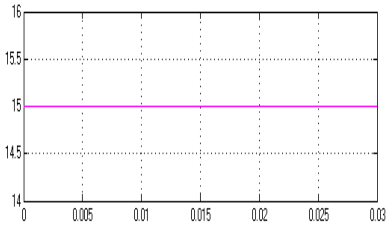


Fig.4(b) : Input Voltage

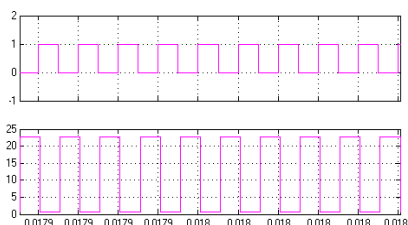


Fig.4(c) : Switching Pulse for M_1 & V_{DS}

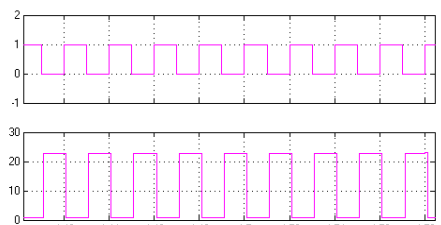


Fig.4(d) : Switching Pulse for M_2 & V_{DS}

Switching Pulse and output voltage for M_2 are shown in Fig.4(d). The voltage source across the MOSFET is a compliment of the driving voltage. The output current of 2.7A and output voltage of 30V are shown in Fig.4(e) and Fig.4(f) respectively. The output power is shown in Fig.4(g) and its value is 85watts.

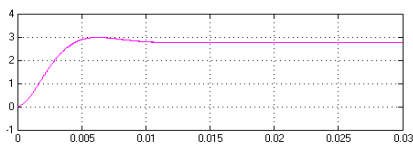


Fig.4(e) : Output Current

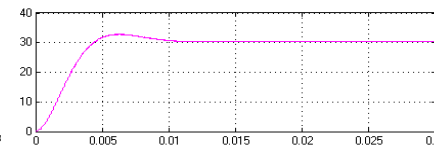


Fig.4(f) : Output Voltage

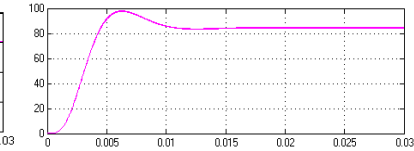


Fig.4(g) : Output Power

The ripple in the output voltage is shown in Fig.4(h). The peak to peak ripple is 0.06Volts.

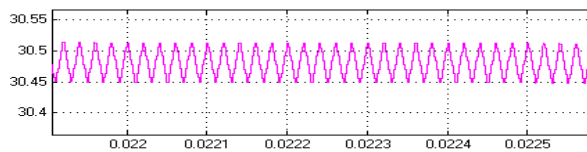


Fig.4(h) : Output Ripple Voltage

The converter in boost mode with pi-filter is shown in Fig.5(a). The simulation parameters for boost mode with Pi-filter are as follows:

Coupled Inductor = 2.1 mH; Pi-filter, $L = 1\mu\text{H}$ and $C_0 = 400\mu\text{F}$ and Resistance, $R_0 = 11\Omega$.

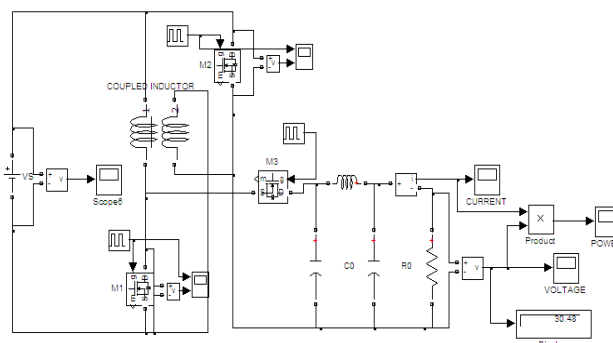


Fig.5(a) : Circuit Diagram for Boost Mode with Pi-Filter

The output current and output voltage of 30V are shown in Fig.5(b) and Fig.5(c) respectively.

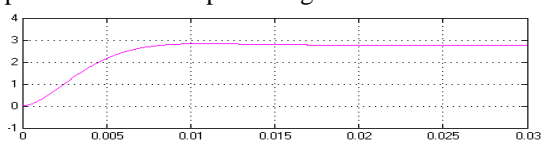


Fig.5(b) : Output Current

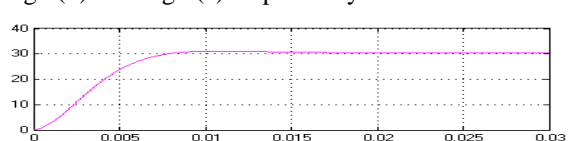


Fig.5(c) : Output Voltage

The output power is 85watts as shown in Fig.5(d). The ripple in the output voltage is shown in Fig.5(e). The peak to peak ripple is 0.01Volts. Thus the ripple is reduced from 0.06V to 0.01V by using pi-filter.

International Journal of Innovative Research in Science, Engineering and Technology

(An ISO 3297: 2007 Certified Organization)

Vol. 4, Issue 2, February 2015

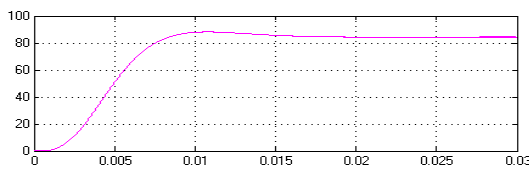


Fig.5(d) : Output Power

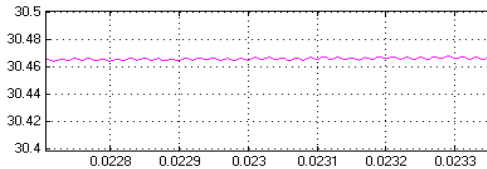


Fig.5(e) : Output Voltage with Reduced Ripple

The circuit diagram for boost mode with motor load is shown in Fig.6(a). The simulation parameter for DC motor load is taken as 240V, 1750 RPM, 5HP and Coupled inductor $L = 1\text{mH}$.

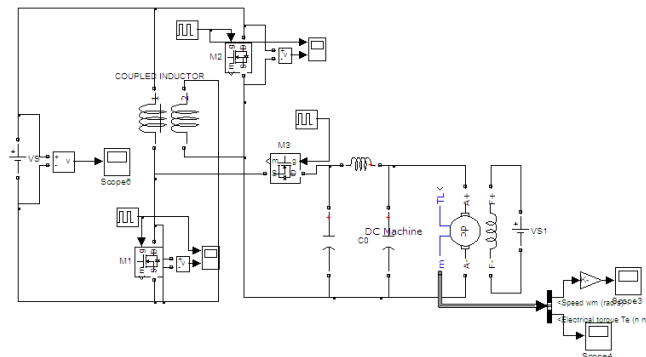


Fig.6(a) : Circuit Diagram with Motor Load

DC input voltage of 15V is shown in Fig.6(b). The speed response is shown in Fig.6(c). The speed settles at 1100rpm. The torque response is shown in Fig.6(d).

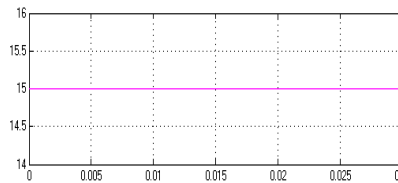


Fig.6(b) : Input Voltage

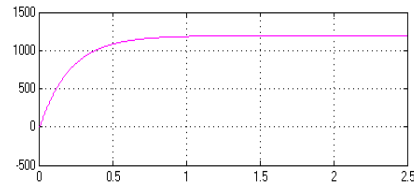


Fig.6(c) : Motor Speed

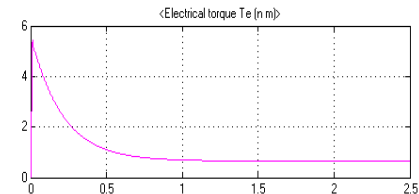


Fig.6(d) : Motor Torque

The converter operating in buck mode is shown in Fig.7(a). The simulation parameters for buck mode with C-filter are as follows: Coupled Inductor = 2.1 mH; C-filter, $C_o = 100\mu\text{F}$ and Resistance, $R_o = 25\Omega$.

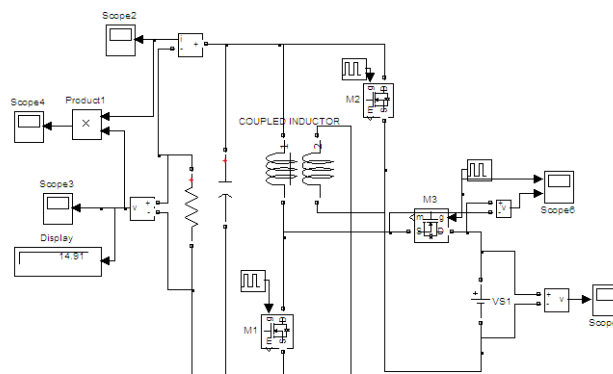


Fig.7(a) : Circuit Diagram for Buck Mode with C-Filter

DC input voltage of 30V is shown in Fig.7(b). Switching Pulse and output voltage for M_3 are shown in Fig.7(c).

International Journal of Innovative Research in Science, Engineering and Technology

(An ISO 3297: 2007 Certified Organization)

Vol. 4, Issue 2, February 2015

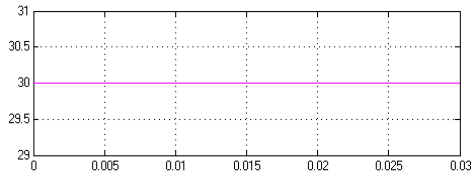


Fig.7(b) : Input Voltage

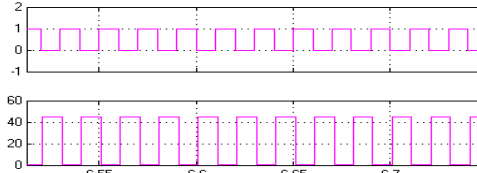


Fig.7(c) : Switching Pulse for M_3 & V_{DS}

The DC output voltage of 14.91V and output current are shown in Fig.7(d) and Fig.7(e) respectively.

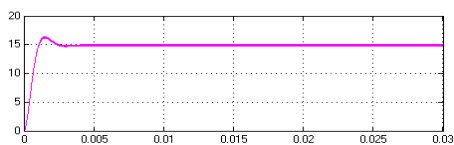


Fig.7(d) : Output Voltage

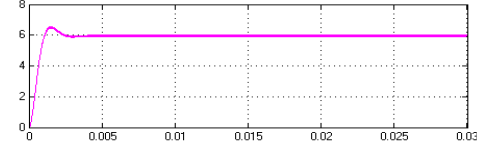


Fig.7(e) : Output Current

The output power is shown in Fig.7(f). The ripple in the output voltage is shown in Fig.7(g).The peak to peak ripple is 0.15Volts.

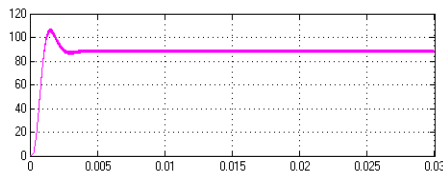


Fig.7(f) : Output Power

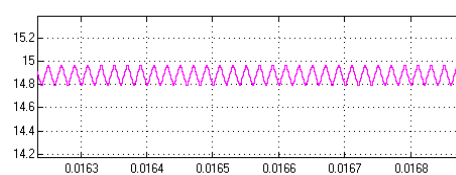


Fig.7(g) : Output Voltage with Reduced Ripple

The circuit diagram for buck mode with pi-filter is shown in Fig.8(a). The simulation parameters for buck mode with Pi-filter are as follows: Coupled Inductor = 2.1 mH, Pi-filter, $L = 1\mu\text{H}$ and $C_0 = 400\mu\text{F}$ and Resistance, $R_0 = 11\Omega$.

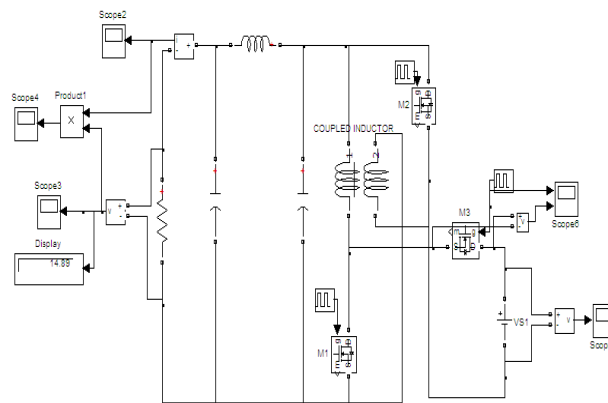


Fig.8(a) : Circuit Diagram for Buck Mode with Pi-Filter

DC input voltage of 30V and output voltage of 15V are shown in Figs.8(b) and 8(c) respectively.

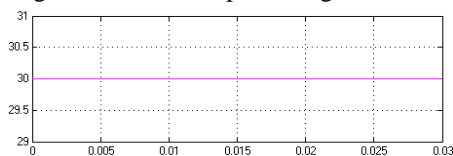


Fig.8(b) : Input Voltage

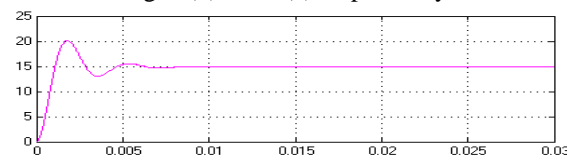


Fig.8(c) : Output Voltage

The output current, output power are shown in Figs.8(d) and 8(e) respectively. The ripple in the output is shown in Fig.8(f). The peak to peak ripple is 0.005Volts.

International Journal of Innovative Research in Science, Engineering and Technology

(An ISO 3297: 2007 Certified Organization)

Vol. 4, Issue 2, February 2015

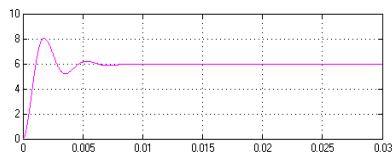


Fig.8(d) : Output Current

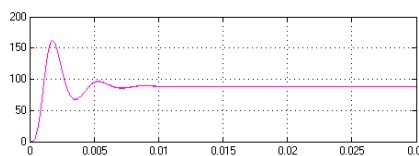


Fig.8(e) : Output Power

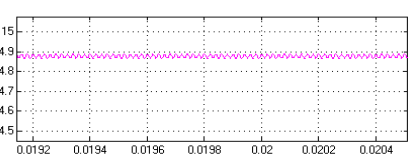


Fig.8(f) : Output Voltage with Reduced Ripple

The circuit diagram in buck mode with motor load is shown in Fig.9(a). The simulation parameter for DC motor load is taken as 240V, 1750 RPM, 5HP and Coupled inductor $L = 2.1\text{mH}$.

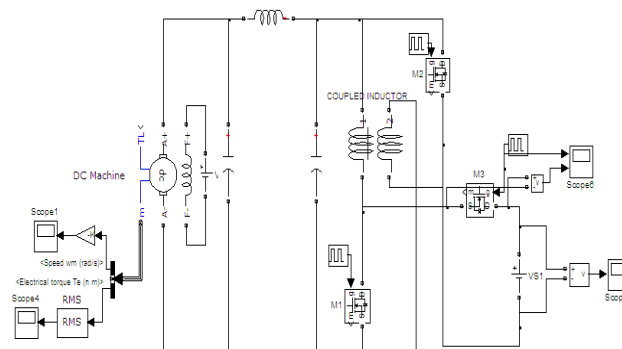


Fig.9(a) : Circuit Diagram with Motor Load

DC input voltage of 30V is shown in Fig.9(b). The motor speed is shown in Fig.9(c).The speed settles at 420rpm. The torque response is shown in Fig.9(d).

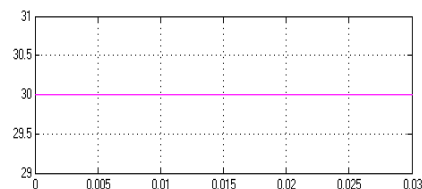


Fig.9(b) : Input Voltage

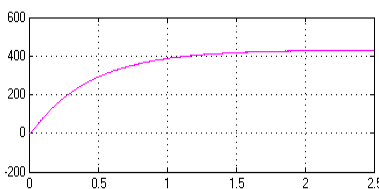


Fig.9(c) : Motor Speed

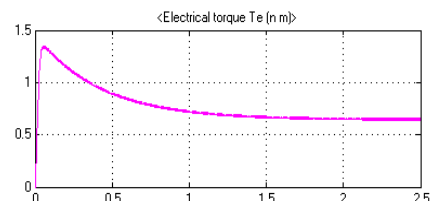


Fig.9(d) : Motor Torque

IV. CONCLUSION

Bidirectional DC-DC converter operating in boost mode and buck mode is simulated successfully with R-load and DC motor load. The ripple in the output voltage is reduced from 0.06Volts to 0.01Volts by using Pi-filter. Therefore the performance of DC motor is improved due to the reduced ripple. The scope of this work is to design and simulate the DC-DC converter using MATLAB. The hardware will be implemented in future. The drawback of this converter is that it can be used only for low power levels.

REFERENCES

- [1] M. B. Camara, H. Gualous, F. Gustin, A. Berthon, and B. Dakyo, "DC/DC converter design for supercapacitor and battery power management in hybrid vehicle applications—Polynomial control strategy," *IEEE Trans. Ind. Electron.*, vol. 57, no. 2, pp. 587–597, Feb. 2010.
- [2] T. Bhattacharya, V. S. Giri, K. Mathew, and L. Umanand, "Multiphase bidirectional flyback converter topology for hybrid electric vehicles," *IEEE Trans. Ind. Electron.*, vol. 56, no. 1, pp. 78–84, Jan. 2009.
- [3] Z. Amjadi and S. S. Williamson, "A novel control technique for a switched-capacitor-converter-based hybrid electric vehicle energy storage system," *IEEE Trans. Ind. Electron.*, vol. 57, no. 3, pp. 926–934, Mar. 2010.
- [4] F. Z. Peng, F. Zhang, and Z. Qian, "A magnetic-less dc–dc converter for dual-voltage automotive systems," *IEEE Trans. Ind. Appl.*, vol. 39, no. 2, pp. 511–518, Mar./Apr. 2003.
- [5] A. Nasiri, Z. Nie, S. B. Bekiarov, and A. Emadi, "An on-line UPS system with power factor correction and electric isolation using BIFRED converter," *IEEE Trans. Ind. Electron.*, vol. 55, no. 2, pp. 722–730, Feb. 2008.
- [6] L. Schuch, C. Rech, H. L. Hey, H. A. Grundling, H. Pinheiro, and J. R. Pinheiro, "Analysis and design of a new high-efficiency bidirectional integrated ZVT PWM converter for DC-bus and battery-bank interface," *IEEE Trans. Ind. Appl.*, vol. 42, no. 5, pp. 1321–1332, Sep./Oct. 2006.

International Journal of Innovative Research in Science, Engineering and Technology

(An ISO 3297: 2007 Certified Organization)

Vol. 4, Issue 2, February 2015

- [7] X. Zhu, X. Li, G. Shen, and D. Xu, "Design of the dynamic power compensation for PEMFC distributed power system," *IEEE Trans. Ind. Electron.*, vol. 57, no. 6, pp. 1935–1944, Jun. 2010.
- [8] G. Ma, W. Qu, G. Yu, Y. Liu, N. Liang, and W. Li, "A zero-voltageswitching bidirectional dc–dc converter with state analysis and softswitching-oriented design consideration," *IEEE Trans. Ind. Electron.*, vol. 56, no. 6, pp. 2174–2184, Jun. 2009.
- [9] F. Z. Peng, H. Li, G. J. Su, and J. S. Lawler, "A new ZVS bidirectional dc–dc converter for fuel cell and battery application," *IEEE Trans. Power Electron.*, vol. 19, no. 1, pp. 54–65, Jan. 2004.
- [10] K. Jin, M. Yang, X. Ruan, and M. Xu, "Three-level bidirectional converter for fuel-cell/battery hybrid power system," *IEEE Trans. Ind. Electron.*, vol. 57, no. 6, pp. 1976–1986, Jun. 2010.
- [11] R. Gules, J. D. P. Pacheco, H. L. Hey, and J. Imhoff, "A maximum power point tracking system with parallel connection for PV stand-alone applications," *IEEE Trans. Ind. Electron.*, vol. 55, no. 7, pp. 2674–2683, Jul. 2008.
- [12] Z. Liao and X. Ruan, "A novel power management control strategy for stand-alone photovoltaic power system," in *Proc. IEEE IPEMC*, 2009, pp. 445–449.
- [13] S. Inoue and H. Akagi, "A bidirectional dc–dc converter for an energy storage system with galvanic isolation," *IEEE Trans. Power Electron.*, vol. 22, no. 6, pp. 2299–2306, Nov. 2007.
- [14] L. R. Chen, N. Y. Chu, C. S. Wang, and R. H. Liang, "Design of a reflexbased bidirectional converter with the energy recovery function," *IEEE Trans. Ind. Electron.*, vol. 55, no. 8, pp. 3022–3029, Aug. 2008.
- [15] S. Y. Lee, G. Pfaelzer, and J. D. Wyk, "Comparison of different designs of a 42-V/14-V dc/dc converter regarding losses and thermal aspects," *IEEE Trans. Ind. Appl.*, vol. 43, no. 2, pp. 520–530, Mar./Apr. 2007.
- [16] K. Venkatesan, "Current mode controlled bidirectional flyback converter," in *Proc. IEEE Power Electron. Spec. Conf.*, 1989, pp. 835–842.
- [17] T. Qian and B. Lehman, "Coupled input-series and output-parallel dual interleaved flyback converter for high input voltage application," *IEEE Trans. Power Electron.*, vol. 23, no. 1, pp. 88–95, Jan. 2008.
- [18] G. Chen, Y. S. Lee, S. Y. R. Hui, D. Xu, and Y. Wang, "Actively clamped bidirectional flyback converter," *IEEE Trans. Ind. Electron.*, vol. 47, no. 4, pp. 770–779, Aug. 2000.
- [19] F. Zhang and Y. Yan, "Novel forward-flyback hybrid bidirectional dc–dc converter," *IEEE Trans. Ind. Electron.*, vol. 56, no. 5, pp. 1578–1584, May 2009.
- [20] H. Li, F. Z. Peng, and J. S. Lawler, "A natural ZVS medium-power bidirectional dc–dc converter with minimum number of devices," *IEEE Trans. Ind. Appl.*, vol. 39, no. 2, pp. 525–535, Mar. 2003.
- [21] B. R. Lin, C. L. Huang, and Y. E. Lee, "Asymmetrical pulse-width modulation bidirectional dc–dc converter," *IET Power Electron.*, vol. 1, no. 3, pp. 336–347, Sep. 2008.
- [22] Y. Xie, J. Sun, and J. S. Freudenberg, "Power flow characterization of a bidirectional galvanically isolated high-power dc/dc converter over a wide operating range," *IEEE Trans. Power Electron.*, vol. 25, no. 1, pp. 54–66, Jan. 2010.
- [23] I. D. Kim, S. H. Paeng, J. W. Ahn, E. C. Nho, and J. S. Ko, "New bidirectional ZVS PWM sepic/zeta dc–dc converter," in *Proc. IEEE ISIE*, 2007, pp. 555–560.
- [24] Y. S. Lee and Y. Y. Chiu, "Zero-current-switching switched-capacitor bidirectional dc–dc converter," *Proc. Inst. Elect. Eng.—Elect. Power Appl.*, vol. 152, no. 6, pp. 1525–1530, Nov. 2005.
- [25] R. J. Wai and R. Y. Duan, "High-efficiency bidirectional converter for power sources with great voltage diversity," *IEEE Trans. Power Electron.*, vol. 22, no. 5, pp. 1986–1996, Sep. 2007.
- [26] L. S. Yang, T. J. Liang, and J. F. Chen, "Transformerless dc–dc converters with high step-up voltage gain," *IEEE Trans. Ind. Electron.*, vol. 56, no. 8, pp. 3144–3152, Aug. 2009.
- [27] Lung-Sheng Yang and Tsorng-Juu Liang, "Analysis and Implementation of novel bidirectional dc-dc converter," *IEEE Trans. Ind. Electron.*, vol. 59, no. 1, Jan. 2012.

BIOGRAPHY



K.C. Ramya has done her B.E from Mailam Engineering College, Mailam, in the year 2002 and M.E from Sathyabama University, Chennai in the year 2010. Presently she is a research scholar at Karunya University, Coimbatore. She is doing her research in the area of bidirectional DC to DC Converters applied to Electrical Vehicles.



Dr. V. Jegathesan has obtained his B.E and M.E degree from Bharathiar University, Coimbatore, India in the year 1999 and 2002 respectively. He obtained his Ph.D from Anna University, Chennai, India in the year 2010. He is presently working as an Associate Professor of EEE Department in Karunya University, Coimbatore, India. He is a fellow member of ISTE, Member of IACSIT and Member of IAENG. He has authored text book on Basic Electrical and Electronics Engineering. He has published various research papers in reputed Journals. His research area includes Electric Circuits and Networks, Power Electronics, Development of Heuristic Algorithms for Power Electronic Applications and Application of Power Electronics to Renewable Energy.